



Stratospheric ozone and QBO interaction with the tropical troposphere on intraseasonal and interannual time-scales: a wave interaction perspective

Breno Raphaldini¹, Andre Seiji Watake Teruya¹, Pedro Leite da Silva Dias¹, Daniel Y. Takahashi², and Lucas Massaroppe¹

¹Department of Atmospheric Sciences, University of Sao Paulo

²Instituto do Cerebro, Federal University of Rio Grande do Norte

Correspondence: Breno Raphaldini (brenorfs@gmail.com)

Abstract. The Madden Julian Oscillation (MJO) is the main controller of the weather in the tropics on intraseasonal time-scales and recent research provide evidences that the Quasi-Biennial Oscillation (QBO) influences the MJO interannual variability. However the physical mechanisms behind this interaction are not completely understood. Recent studies on the normal mode structure of the MJO indicates the contribution of global scale Kelvin and Rossby waves. In this study we test whether these MJO-related normal modes are affected by the QBO and stratospheric ozone. The Partial Directed Coherence method enabled us to probe the direction and frequency of the interactions. It was found that the tropical stratosphere influences the MJO, with ozone and stratospheric wind influencing the MJO at periods of 1-2 months and 1.5-2.5 years, and on the decadal time-scale, the latter probably related to solar cycle forcing. We explore the physical mechanisms behind the stratosphere-troposphere interactions by performing a linear regression between the MJO/QBO indices and the amplitudes of the normal modes of the atmosphere obtained by projections on a normal mode basis using ERA-Interim reanalysis data. The MJO is dominated by symmetric Rossby modes but is also influenced by Kelvin and asymmetric Rossby modes. The QBO is mostly explained by westward propagating inertio gravity waves and asymmetric Rossby waves. We explore the previous results by identifying interactions between those modes and between the modes and the ozone concentration. In particular, westward inertio-gravity waves, associated with the QBO, influences the MJO on interannual time-scales. These modes have their largest intensities above the Himalayas in the stratosphere, suggesting that this region plays a key role in the QBO-MJO interaction.

1 Introduction

The Madden Julian Oscillation (MJO) and the quasi-biennial oscillation (QBO) are two of the main elements of the atmospheric low frequency variability in the tropics. The MJO acts on intraseasonal time-scales on the troposphere and is determinant for the tropical monsoons and with global impacts (Zhang, 2005). The QBO manifests in the tropical stratosphere as a reversal



of the zonal winds with downward propagation cycles with mean period of 28 months. Both are important players for the Earth system's weather and climate. Careful examination of causal relationships between such processes and inference of the dominant frequencies and the physical mechanisms behind their interaction are active topics of research in recent years (Zhang *et al.*, 2018).

5 An important aspect of the stratospheric influence on the troposphere comes from the fact that it can comprise a pathway for the impact of the solar variability in the troposphere. It is conjectured that stratospheric influence on the troposphere exists via the so-called top-down mechanism (Gray *et al.*, 2010). According to this hypothesis, stratospheric ozone absorbs ultraviolet solar (UV) radiation releasing heat. This heat then generates temperature and wind perturbations in the stratosphere that might then induce a tropospheric response through downward energy transport. However, details of the physical mechanisms through
10 which stratospheric signals could propagate down to the troposphere are not completely understood.

Stratospheric control of tropospheric phenomena in mid to high latitudes was addressed in several papers. For instance, Baldwin *et al.* (2010) highlights the polar vortex as an important example of such control. Another example is that of stratospheric impacts on tropospheric upper level jets and storm tracks as seen in Kidston *et al.* (2015). Yoo & Son (2016) showed that the MJO depends on the QBO phase in the annual timescale, concluding that including QBO information improves the MJO
15 predictability (Marshall *et al.*, 2017; Son *et al.*, 2017). Densmore *et al.* (2019) attributes differences on the QBO-MJO interaction depending on the QBO phase to differences in the static stability of the upper troposphere/lower stratosphere, leading to changes in the excitation of MJO-related disturbances. Hendon & Abhik (2018) associated the increased predictability and intensity of the MJO during the boreal winter and QBO easterly phase with differences in the vertical structure of the MJO, depending on the QBO phase. The problem of MJO-QBO connection is however still not well understood from the perspective
20 of the underlying physical mechanism nor well represented in numerical models as pointed out recently in .

Recent series studies have given a normal mode description of the MJO (Zagar & Frankze, 2015; Kitsios *et al.*, 2019). These studies concluded that the MJO can be described as global scale baroclinic Rossby and Kelvin waves. The same approach was used to study the circumstances that lead to the 2016 QBO disruption (Raphaldini *et al.*, 2020). In this context a natural question arises: what is the role of these normal modes in the MJO interaction with the stratosphere? In particular, how these modes
25 interact with QBO-related modes?

In this article, we study the interactions between the stratosphere and the tropical troposphere, with particular emphasis on the MJO. A time series analysis causality method, Partial Directed Coherence (PDC), (Baccala & Sameshima, 2001) was used. We determine whether equatorial ozone, equatorial stratospheric zonal winds and tropospheric fields interact and how this interaction occurs, including information on directional interaction. Our analysis is based on daily data of stratospheric
30 zonal wind, ozone concentration, and the unfiltered MJO index from 1979 to 2015. We obtained stratospheric zonal wind and ozone concentration from ERA-Interim reanalysis data (Dee *et al.*, 2011) from the European Center for Mid-Range Weather Forecasts. Zonal wind at 30 hPa level was averaged in an equatorial belt from -15° to 15° latitude for all longitudes, which is a reasonable choice to represent the QBO (Nappo, 2013). Ozone data were averaged from -20 to 20 in latitude and integrated for all levels from 100 to 0.1hPa. MJO data was obtained from the daily MJO index RMM (Wheeler & Hendon, 2004). The
35 MJO index is presented in a polar coordinate diagram with two time-series, for the amplitude and phase. The amplitude of the



MJO index is defined as the sum of the squares of the first two empirical orthogonal functions (EOFs) of combined pressure fields at 200 and 850hPa and outgoing long wave radiation data in the tropics (RMM1 and RMM2). An equivalent way to represent the MJO index (a complex number) is to use two real variables that correspond to the two first components. Here we use this last representation. The reason for this choice is that the squaring operation can distort the power spectrum by generating artificial frequencies by frequency doubling. Since the statistical analysis relies on the estimation of the spectrum, using separated EOFs gives more accurate results.

To resolve the spectrum of the different time-scales, time-scale separation was applied to the data. We split the data into a fast time-scale (periods shorter than one year), and a slow time-scale (periods greater than one year). This was done by performing a moving average on the data with a ten-day rate for the "fast" time-scale. A six-month window was applied for the "slow" time-scale.

The causality between the QBO, tropical stratospheric ozone and the MJO, was studied using the PDC method. PDC corresponds, roughly, to a frequency domain counterpart of the Granger Causality test (Baccala & Sameshima, 2001), with the additional advantage of providing information on the specific frequencies at which the causality occurs.

We seek for physical mechanisms that might be responsible for interactions between stratospheric and tropospheric phenomena by performing a linear regression with the MJO indices and stratospheric zonal winds. We then perform the PDC analysis with the time series for the energies associated with each of the Hough modes responsible for the MJO dynamics (as in Zagar et al. (2015)) and of the stratospheric zonal wind. The results indicate that the interaction of internal westward gravity waves, responsible for the QBO and Kelvin, and Rossby waves associated with the MJO, partially explain the stratospheric influences on the MJO.

20 2 Methods

2.1 Granger Causality

The concept of causality is a central question in science. One possible definition of causality related to the predictability of two or more distinct processes was introduced in Granger (1969) and is currently known as Granger causality in the literature. The main advantage is the ability to pinpoint the direction of interaction, unlike other measures such as coherence, correlation, partial coherence and partial correlation. The following definition is specific to trivariate time series but is readily generalizable to an arbitrary number of time series.

Consider a vector-valued signal $\mathbf{X}(t) = [X_1(t), X_2(t), X_3(t)]^\top$ where the superscript \top indicates the transpose of a vector and $\mathbf{X}(t)$ is assumed to have a vector autoregressive representation of order p (hereafter referred as VAR(p))

$$\begin{bmatrix} X_1(t) \\ X_2(t) \\ X_3(t) \end{bmatrix} = \sum_{k=1}^p \begin{bmatrix} a_{11}(k) & a_{12}(k) & a_{13}(k) \\ a_{21}(k) & a_{22}(k) & a_{23}(k) \\ a_{31}(k) & a_{32}(k) & a_{33}(k) \end{bmatrix} \begin{bmatrix} X_1(t-k) \\ X_2(t-k) \\ X_3(t-k) \end{bmatrix} + \begin{bmatrix} \epsilon_1(t) \\ \epsilon_2(t) \\ \epsilon_3(t) \end{bmatrix}, \quad (1)$$



where $a_{ij}(k)$ are the $\text{VAR}(p)$ coefficients representing the k -th lagged influence of the j -th component of the signal on the i -th component and t denotes the time variable. The innovations processes $\epsilon_i(t)$ has zero mean and covariance matrix $\mathbf{C} = [\sigma_{ij}]$, such that $\text{Cov}(\epsilon_i(t), \epsilon_j(s)) = 0$ for $t \neq s$ and for all $i, j \in \{1, 2, 3\}$.

It is enough to say that $X_j(t)$ Granger causes $X_i(t)$ for $i \neq j$ if $a_{ij}(k) \neq 0$, for some lag $k = 1, \dots, p$. Thus, the absence of
 5 Granger causality from $X_1(t)$ to $X_2(t)$ implies that $X_1(t)$ does not help to predict $X_2(t)$, once the past of $X_2(t)$ and $X_3(t)$ are considered.

In practice, given a trivariate time series $\mathbf{X}(t)$ of length n , we estimate the $\text{VAR}(p)$ model from the data and test for $a_{ij}(k)$ nullity. More precisely, the idea is verify the null hypothesis

$$\mathcal{H}_0 : a_{ij}(k) = 0, \quad k = 1, \dots, p, \quad (2)$$

10 against

$$\mathcal{H}_1 : \text{there exist } k \in \{1, \dots, p\}, \text{ such that } a_{ij}(k) \neq 0. \quad (3)$$

In summary, we can say that the j -th component of the time series causes the i -th component in the sense of Granger if the past of the j -th component helps to predict the future of the i -th component. We have used the MATLAB Toolbox (free) implementation of the $\text{VAR}(p)$ and Granger causality estimators implementations from *Sameshima et. al.* (2015), available at
 15 <http://www.lcs.poli.usp.br/~baccala/pdc>.

2.2 Partial directed coherence

Partial Directed Coherence (PDC) is an extension of the concept of Granger causality to the frequency domain, as a measure of information flow. Thus, PDC incorporates advantages of both former methods with the additional advantage that it can be generalized to more than two time series enabling to explicitly pinpoint the directed information flow from mere indirect
 20 interactions, (*Baccala & Sameshima, 2001; Takahashi et. al., 2007, 2010*). PDC has been successfully applied in complex systems as neuroscience (*Baccala & Sameshima, 2001; Schelter et. al., 2006*) and economics (*Hui & Chen, 2012*). PDC was also used to detect the causality between the El Niño Southern Oscillation and the monsoons and also in the sea-air interaction in the South Atlantic Convergence Zone (*Tribassi et. al, 2017*).

Again, consider a trivariate time series $\mathbf{X}(t) = [X_1(t), X_2(t), X_3(t)]^\top$ with a $\text{VAR}(p)$ representation defined in (1), let

$$25 \quad \bar{A}_{kl}(\nu) = \delta_{kl} - \sum_{s=1}^p a_{kl}(s) e^{-i2\pi\nu s}, \quad (4)$$

where δ_{kl} is the Kronecker delta symbol, $i^2 = -1$, ν the Fourier frequency (in Hertz), s the time (in seconds). Here we use the more general PDC definition, the information-Partial Directed Coherence (${}_i\text{PDC}$), which is closely related to information theory. It has been shown that ${}_i\text{PDC}$ corresponds to the information flow (in Shannon's sense) between different signals (*Baccala et. al., 2013*). Therefore the information flow, ${}_i\text{PDC}$, from $X_j(t)$ to $X_i(t)$ in a specific frequency $\nu \in [-1/2, 1/2)$, is given by

$$30 \quad {}_i\text{PDC}_{i \leftarrow j}(\nu) = {}_i\pi_{ij}(\nu) = \frac{\bar{A}_{ij}(\nu) / \sqrt{\sigma_{ij}}}{\sqrt{\bar{\mathbf{a}}_j^H(\nu) \mathbf{C}^{-1} \bar{\mathbf{a}}_j(\nu)}}, \quad (5)$$



where $\bar{\mathbf{a}}_j(\nu)$ is the j -th column of the matrix with coefficients $\bar{A}_{kl}(\nu)$, and $\bar{\mathbf{a}}_j^H(\nu)$ denotes its Hermitian transpose.

Note that there is a duality between the Granger causality and PDC, as demonstrated in *Sameshima et al. (2015)*. Therefore the nullity of ${}_i\pi_{ij}(\nu)$ corresponds to the absence of connection (similarly to the aforementioned Granger causality condition), which, in the PDC case, also has a rigorous and well-defined statistical criterion for the null hypothesis test (*Baccala et al., 2013*). Confidence intervals for the PDC analysis are explicitly calculated as the statistics of the PDC coefficients, ${}_i\pi_{ij}(\nu)$, is asymptotically Gaussian (at the limit of a large number of data points). For a proof of this theorem and more information on confidence intervals for PDC see *Baccala et al. (2013)* and *Takahashi et al. (2007)*. To estimate the ${}_i$ PDC from the data, the first step is to obtain the vector autoregressive model, which is estimated through the Hannan-Quinn criterion in this paper and substitutes the estimated coefficients in Eq.(3). The implemented test statistics are described in *Baccala et al. (2013)*, and we used the computations of ${}_i$ PDC generated from AsympPDC Package version 3.0 MATLAB Toolbox freely available as mentioned before. A detailed example showing how to interpret the PDC plots is given in the supplementary material (see figure S1).

The partial directed coherence technique as well as Granger causality related techniques are linear in nature and a natural question is whether these technique are able to capture the interaction between signals that arise from nonlinear problems. There are several publications addressing this question such as possible nonlinear extension of this technique (*Massaroppe & Baccala, 2015; Wahl et al., 2016*) and the introduction of other techniques that are intrinsically nonlinear in nature, based on time lagged embedding, such as *Sugihara et al. (2012)*, or based in the concept of Markov partitions, such as *Bianco-Martinez et al. (2018)*. *Sugihara et al. (2012)* gives an example in which Granger based techniques perform poorly. Here we argue that although PDC does not capture all kinds of nonlinear coupling between time scales specially with more intermittent/non-Gaussian behavior, it certainly capture certain kinds of nonlinear interactions. As proved in *Takahashi et al. (2010)* there is an equivalence between the concepts of mutual information rate that would account for all information flow between two or more signals and PDC, in the case of Gaussian processes. In the general non-Gaussian case bounds are given for the difference of the mutual information rate estimated by PDC and the actual mutual information rate, meaning that even if the signals are non-linear and non-Gaussian PDC is still able to capture part of the information flow between the signals.

2.3 Normal mode decomposition

Zagar et al. (2015), based on the methodology of *Kasahara & Puri (1981)*, introduced a software for the projection of observed atmospheric fields onto the normal modes of the hydrostatic primitive equations on the sphere. For a vector valued function $\mathbf{X} = [u, v, h]^T$, where $u(\lambda, \phi, z)$ is the zonal velocity field, $v(\lambda, \phi, z)$ is the meridional velocity field, $h(\lambda, \phi, z)$ is the modified geopotential height. A separation of variables is then performed and the state vector \mathbf{X} is represented as a series of horizontal and vertical structure functions, which in discrete form is

$$\mathbf{X}(\lambda, \phi, z) = \sum_{m=1}^M \mathbf{S}_m \mathbf{X}_m(\lambda, \phi) G_m(z), \quad (6)$$



where \mathbf{X}_m is the horizontal structure vector function, G_m is the vertical structure function and \mathbf{S}_m is a square matrix defined as

$$\mathbf{S}_m = \begin{bmatrix} \sqrt{gD_m} & 0 & 0 \\ 0 & \sqrt{gD_m} & 0 \\ 0 & 0 & D_m \end{bmatrix},$$

where g is Earth's gravity and D_m equivalent depth of the m -th vertical mode. The horizontal fields \mathbf{X}_m , on the other hand, are expanded in Hough harmonics as

$$\mathbf{X}_m(\lambda, \phi) = \sum_{n=1}^N \sum_{k=-K}^K \chi_{m,n,k} \mathbf{H}_{m,n,k}(\lambda, \phi), \quad (7)$$

where $\mathbf{H}_{m,n,k}$ are the eigenfunctions of the Laplace's tidal equation considering zonal periodicity and regularity at the poles as boundary conditions (Longuet-Higgins & Selwyn, 1968). The expansion coefficients $\chi_{m,n,k}$ are obtained as

$$\chi_{m,n,k} = \frac{1}{2\pi} \int_0^{2\pi} \int_{-1}^1 \mathbf{X}_m(\lambda, \phi) \cdot [\mathbf{H}_{m,n,k}(\lambda, \phi)]^* d\mu d\lambda, \quad (8)$$

with $\mu = \sin(\phi)$ and the superscript * indicates the complex conjugate. Details of the procedures for obtaining the amplitudes $\chi_{m,n,k}$ from the data is described in Zagar *et al.* (2015). The MODES software then provides the amplitudes $\chi_{m,n,k}$ given input time scales of reanalysis data. Zagar & Frankze (2015) proposed a procedure to decompose the MJO into the contributions of each normal mode by performing a linear regression between the MJO time series and the mode-amplitude time series

$$\mathcal{R}_{m,n,k} = \frac{1}{N-1} \sum_{t=1}^N \frac{(\chi_{m,n,k}(t) - \mathbf{E}[\chi_{m,n,k}(t)])(Y(t) - \mathbf{E}[Y(t)])}{\text{Var}[Y(t)]} \quad (9)$$

where $\chi_{m,n,k}(t)$ is the Hough expansion coefficient (8) for a time instant t , $Y(t)$ is the MJO index time series and $\mathbf{E}[Y(t)]$ and $\text{Var}[Y(t)]$ are the respective expectation and variance, respectively.

3 Statistical analysis: QBO-MJO-Ozone interaction

The results for the fast time-scale (20 – 180 days). The time series were well-adjusted by the autoregressive vector model, passing the Portmanteau test (Lutkepohl, 2005). The PDC analysis (Figure 1) indicates that there is a statistically significant interaction between the stratospheric mean zonal wind and the MJO and between tropical stratospheric ozone and the MJO. First, the interaction between the two MJO indices was found to interact at most frequencies, as expected. Influence from RMM1 and RMM2 on stratospheric mean zonal wind is found to occur during periods in the intraseasonal time-scale, at the lower frequency MJO range, with time-scales of around 50 and 90 days, which might be a result of the effects of deep convection on the stratosphere (Tian *et al.*, 2007). Concerning the influence of the stratospheric variables on the MJO, tropical stratospheric ozone is shown to have a significant influence on RMM1 and RMM2, influencing RMM1 during periods of



around one month, corresponding to the higher frequency MJO cycle, and RMM2 throughout the whole intraseasonal time scale. The periods when ozone influences RMM1 and RMM2 show, by the definition of Granger Causality, that information on ozone should improve the MJO predictability. Significant directional interaction is found from stratospheric zonal wind to RMM1 and RMM2 at 20 – 30 days, and particularly to RMM1 on six-month time-scales, possibly as a subharmonic of the annual cycle.

Finally, we investigated the interaction between the stratospheric variables. Tropical stratospheric ozone is found to strongly influence the stratospheric zonal wind on intraseasonal time-scales and on a six-month time-scale, possibly as a subharmonic of the annual cycle (i.e. the Sun passes over the equator twice a year). We performed four separate bivariate analyses on the slow time-scale instead of analyzing all the time-series together, and as we have used a 6-month sliding window, the number of data points is too low to reliably fit a quadrivariate autoregressive model. All the time series were well fitted by the multivariate autoregressive models according to the Portmanteau test. Ozone is found to significantly influence the MJO, what can be seen in Figure 2, on the annual time-scale for RMM2, possibly due to the annual cycle, and on the time-scale of 1.6 – 2.1 years, possibly associated with the QBO. Both RMM1 and RMM2 are found to be significantly affected at frequencies with a peak at 11 years, what is a strong indication of the effect of the solar cycle on the MJO, through ozone, which could explain the solar cycle related monsoon variability (VanLoon & Meehl, 2012). Finally, in the slow time-scale, it was found that the stratospheric zonal wind had a significant impact on RMM1 and RMM2 (Figure 3). Interactions that are significant are found from ozone to the MJO in a period ranging from one to two years, possibly as a combination of effects of the annual cycle and the QBO, corroborating the recent results in the literature (Marshall *et. al.*, 2017; Son *et. al.*, 2017; Yoo & Son, 2016).

4 Modal decomposition and wave interactions

In order to search for physical mechanisms that might account for the results described in the previous section we initially perform a linear regression analysis between the time series associated with the MJO indices and to the stratospheric zonal wind representative of the QBO, aiming to find which normal modes best represent such oscillations.

The first step is to perform the analysis of Zagar *et. al.* (2015) to check if the MJO indices RMM1 and RMM2 are in fact dominated by the balanced (Rossby) modes. Zagar & Frankze (2015) showed that the dominant modes in the decomposition are the symmetric Rossby mode (with the largest contribution coming from the Rossby mode with meridional index 1, denoted by RSSY1), as well as Kelvin waves (KW). Both Kelvin and Rossby modes have larger regression coefficient for the vertical mode indices 5-9, which have a first baroclinic structure in the troposphere. In Figure 4 we present the reconstruction of the MJO structure in the physical space, obtained by summing the normal mode functions with largest regression coefficients, in accordance with the analysis of (Zagar & Frankze, 2015).

We performed a similar analysis with the daily time-series of equatorial zonal wind at 30 hPa which is dominated by the QBO. We find that the dominant modes in our regression analysis are westward propagating gravity waves (WIG) and the first asymmetric Rossby modes (meridional index 2, denoted by RWASY1). The reconstruction in physical space of the zonal wind in a plane crossing the equator is shown in Figure 5.



We seek for interactions between the MJO and QBO normal modes. In order to do so, we calculate the time-series of the energy associated with each of the modes (i.e. a weighted sum of the square of absolute value of each of the modes). We begin by describing the interaction between modes associated with the MJO and to the QBO and tropical stratospheric ozone forcing on sub-annual time scales. Due to the large number of variables we split the analysis into three sets, each containing all the “stratospheric variables” against one of the variables associated with the MJO. Since the most important interactions between QBO modes and MJO modes are through the QBO-related WIG waves, we restrict the analysis to these modes.

In Figure 6 we present the PDC analysis of the interaction of Kelvin wave vs. westward inertio-gravity wave vs. stratospheric ozone vs. asymmetric Rossby wave, the first three variables associated with stratospheric phenomena and the last one associated with the MJO. We observe that the ozone forcing acts directly on the MJO related Kelvin waves, most notably on intraseasonal time-scales, with a peak around 50 days. The influence of ozone on this mode is also relevant on a semi-annual and annual time-scale both associated to the annual cycle. WIG waves are found to influence the Kelvin waves on the time-scale of 30 days, while asymmetric Rossby waves are found to influence the Kelvin waves on time-scales from around 50 days to the semi-annual and annual time-scales. We find a feedback from the Kelvin wave to the stratospheric-related variables on intraseasonal, semi-annual and annual time-scales.

Finally, we perform the PDC analysis of the interaction between symmetric Rossby wave (the dominant mode on the MJO decomposition), asymmetric Rossby wave, WIG wave and stratospheric ozone on the fast time-scale. The corresponding PDC plot is presented in Figure 7. The influence of stratospheric ozone on symmetric Rossby waves has peaks at 40 days, 60 days and on a semi-annual time-scale. The influence of the modes associated to the stratospheric zonal wind on the MJO-related Rossby mode seems to be significant throughout the entire intraseasonal time-scale range, most notably around 30 – 40 days, as well as on semi-annual and annual time-scales. Similarly to the previous cases, the feedback of the MJO-related mode to the stratospheric-related variables takes place on intraseasonal, semi-annual and annual time-scales.

We proceed by analyzing the PDC between the modes associated with stratospheric zonal wind and stratospheric ozone vs MJO-related modes on slow time-scales (annual-decadal time-scales). Most importantly, we search for stratospheric influences on MJO on decadal and biennial time-scales. The analysis of the interaction between Kelvin waves, associated with the MJO and tropical stratospheric ozone is presented in Figure 8. It shows that there is a significant causality from ozone to Kelvin waves on a decadal time-scale. Given that both spectra have a peak on the decadal time-scale we can say that the ozone, which is directly influenced by the solar variability, has a peak directly associated with the solar-cycle and the peak on the Kelvin wave spectrum is at least partially explained by the influence of the ozone on it. Kelvin waves on the other hand influence the ozone on annual time-scales, probably due to the annual cycle. The analysis of the interaction between gravity waves associated with the stratospheric zonal wind and the MJO-related Kelvin waves is presented in Figure 9. We found an important influence of the westward inertio-gravity waves on the Kelvin waves on biennial time-scales and on decadal time-scales. The first one is clearly associated with the biennial peak on the inertio-gravity wave spectrum which is a product of the quasi-biennial oscillation and might be associated to the results of *Yoo & Son* (2016) and subsequent articles on the relationship between the QBO and the MJO. The PDC peak on the decadal time-scale is possibly associated with the solar cycle and the gravity modes are forced by the ozone (Figure 11). Since we do not find spectral peaks on this range, we suspect that this is related to the nearest peak,



which is annual. A strong causality is also found on a decadal time-scale, again probably due to the solar cycle. The influence of WIG modes on the MJO related Rossby modes is presented in Figure 10, showing a influence of WIG modes on Rossby modes on annual and biennial timescales.

4.1 Spatial structure of the barotropic WIG waves

5 Considering that the WIG modes are responsible for a large part of the QBO-MJO interaction, it is then important to investigate how these waves manifest in physical space. We recompose the zonal wind field u of WIG waves associated with the QBO (with barotropic structure on the troposphere and baroclinic structure on the stratosphere). Figure 12 shows the zonal wind near 100 hPa, and the vertical structure of the zonal wind is shown in Figure 13. We observe that these waves have their maximum intensity near the Himalayas, and in the vertical direction the maximum intensity of these waves is observed at the
10 stratosphere. This suggests that the inertio-gravity waves linked to the topography in the Himalyas region play an important role in the QBO-MJO interaction. The latitudinal position of the maxima of WIG waves suggests that the well-known tropic-extra tropics interaction mechanism (*Raupp et al.*, 2008) for initiation of the MJO could be relevant here.

Regions of intense WIG waves, such as the Himalayas and North America coincide with regions of occurrence of cold outbreaks, which are known to be influenced by stratospheric phenomena (*Kretschmer et al.*, 2018). The amplitudes of these
15 WIG waves are stronger in the boreal winter and weaker in the boreal summer (not shown here). This is also a possible reason for a stronger QBO-MJO connection in the boreal summer.

5 Final remarks

The PDC results show strong coupling between tropical ozone, stratospheric zonal wind and the MJO. Most notable are the effects of tropical stratospheric winds and ozone influencing the MJO on both intra- and interannual time-scales. The
20 PDC analysis shows that the tropical stratospheric ozone influences the MJO in periods of 30 – 60 days, 1.5 – 2 years, and 10 – 11 years. The first period agrees with the MJO period range, suggesting that stratospheric ozone may play a role in the MJO dynamics. The second roughly agrees with the QBO period and the third suggests a solar cycle influence on the MJO. Stratospheric zonal winds also influence the MJO during periods that fall into the QBO period range, in agreement with the recent results of *Yoo & Son* (2016), who showed that there is an interannual variability in the MJO amplitude that depends on
25 the QBO phase. Marshall (2016) also shows that the QBO explains up to 40% of the MJO interannual variability in the boreal winter (also see *Son et al.* (2017)).

By the definition of Granger causality, one signal causes a second signal if the information of the first helps to predict the future of the other, after taking into account the past of the second signal. In this sense, we confirm the results of the recent studies cited above. We also show that tropical stratospheric ozone also improves the MJO predictability on interannual and
30 decadal time-scales. The periods of interaction suggest that the QBO might be an important process in troposphere/stratosphere coupling through MJO. This conclusion agrees with numerical studies such as that of *Meehl et al.* (2009), stressing the importance of a realistic QBO in coupled troposphere-stratosphere models. We note that ozone influences the MJO on the



intraseasonal time-scales, raising the possibility of tropical stratospheric ozone fluctuations contributions to the initiation of the MJO cycle. On the decadal time-scale, ozone and QBO are modulated by solar activity and ozone was shown to have important impacts on the MJO in this time-scale. There is strong evidence in the literature for the solar cycle impact on the Asian monsoons from both instrumental observations and palaeoclimatic reconstruction, with the rainfall rate in the Indian subcontinent increasing by up to 20% during the solar maximum (*VanLoon & Meehl, 2012*). Since monsoons are linked to the MJO, especially in the Indian region where the MJO signal is strongest, it would be natural to hypothesize that the MJO is a mediator between solar variability and monsoons.

It was also found that the MJO can affect stratospheric ozone, a possible mechanism for this being the impact of deep convection on the tropopause height (*Tian et. al., 2007*). Another interesting question is whether the relationship between the MJO and the QBO is affected by the recent anomalous behavior of the QBO (*Osprey et. al., 2016; Raphaldini et. al., 2020*).

As for physical mechanisms that could link stratospheric heating, driven by solar UV forcing, and tropical convection, investigation on tropopause changes caused by ozone absorption is a possible candidate. *Kang et. al. (2011)* suggested a polar latitudes mechanism associated with changes of wave momentum flux due to ozone depletion associated with the ozone hole. Although this mechanism was proposed for high latitudes, it would be interesting to investigate whether it can be extended to the tropics and to ozone changes due to the annual and solar cycles. Recently, *Lu et. al (2017)* suggested that changes in the wave-guides of planetary waves in the stratosphere, caused by solar forcing changes in the mean flow of the stratosphere, might cause downward planetary wave reflection in high solar activity conditions.

We performed a linear regression analysis of the MJO-index and stratospheric zonal winds against the time-series of the amplitudes of the Hough modes. We confirm that the MJO is explained mainly by the first symmetric Rossby Mode (meridional index 1), Kelvin modes, in agreement with *Zagar & Frankze (2015)*. The stratospheric zonal wind variability is explained mainly by the WIG modes and the first asymmetric Rossby modes (meridional index 2). We analyzed the interaction among those variables and tropical stratospheric ozone. The exchange of energy between the modes and their interaction with the ozone forcing explains the previous results. We highlight the strong influence of the ozone on the MJO-related modes on the intraseasonal time scale and on decadal time-scales, the last one being possibly a result of the solar cycle. We found influences of the gravity modes on the MJO-related modes to be the most relevant on bi-annual time-scales. This explains at least partially the work of *Yoo & Son (2016)* as well as subsequent articles on the QBO-MJO relation. The spatial manifestation of these WIG modes reveals a intense pattern near the Himalayas. This pattern is stronger in the borel winter, leading to a stronger stratospheric impact on the MJO in this season.



Author contributions. B.R. proposed the study, wrote the manuscript and did the statistical analysis, D.Y.T and L.M. worked on the PDC analysis, A.S.T. performed the normal mode decomposition analysis, P.L.S.D. helped with the discussion and the interpretation of the analysis.

Competing interests. The authors declare that they have no conflict of interest.

Acknowledgements. This work was financed by the FAPESP-PACMEDY project (grants 2015/50686-1 and 2017/23417-5) and CAPES IAG/USP PROEX (grant 0531/2017).



References

- Amos, D.E. ; Koopmans, L.H., Tables of the distribution of the coefficient of coherence for stationary bivariate Gaussian processes, Sandia Corporation, 1963.
- Baccala, L.A., Sameshima, K. Overcoming the limitations of correlation analysis for many simultaneously processed neural structures. Prog. Brain Res. 130, 33-47 (2001).
- 5 Baccala L, De Brito C, Takahashi D, Sameshima K, Unified asymptotic theory for all partial directed coherence forms. Philos Trans R Soc A 371:1–13, 2013.
- Baldwin MP, Gillett NP, Forster P, Gerber EP, Hegglin MI, Karpechko AY, Kim J, Kushner PJ, Morgenstern OH, Reichler T. (2010) Effects of the Stratosphere on the Troposphere (Chapter 10), WMO/ICSU/IOC World Climate Research Programme. *World Climate Research Programme.* ,
- 10 BIANCO-MARTINEZ, Ezequiel; BAPTISTA, Murilo S. Space-time nature of causality. Chaos: An Interdisciplinary Journal of Nonlinear Science, v. 28, n. 7, p. 075509, 2018.
- Dee, D. P., et al. , The ERA-Interim reanalysis: configuration and performance of the data assimilation system, Q. J. R. Meteorol. Soc., 137(656), 553 - 597,2011.
- 15 Densmore, Casey R.; Sanabia, Elizabeth R.; Barrett, Bradford S. QBO influence on MJO amplitude over the Maritime Continent: Physical mechanisms and seasonality. Monthly Weather Review, v. 147, n. 1, p. 389-406, 2019.
- Diallo, M., Riese, M., Birner, T., Konopka, P., Müller, R., Hegglin, M. I., ... & Ploeger, F. (2018). Response of stratospheric water vapor and ozone to the unusual timing of El Niño and the QBO disruption in 2015–2016. Atmospheric Chemistry and Physics, 18(17), 13055-13073.
- Feldstein, S. B. and Lee, S., 2014: Intraseasonal and Interdecadal Jet Shifts in the Northern Hemisphere: The Role of Warm Pool Tropical Convection and Sea Ice. J. Climate, 27, 6497-6518.
- 20 Freitas, A. C. V. ; Aimola, L. ; Ambrizzi, T. ; de Oliveira, C. P. . Changes in intensity of the regional Hadley cell in Indian Ocean and its impacts on surrounding regions, v. 43, p. 1245-1253, 2016.
- Kretschmer, M., Cohen, J., Matthias, V., Runge, J., & Coumou, D. (2018). The different stratospheric influence on cold-extremes in Eurasia and North America. npj Climate and Atmospheric Science, 1(1), 44.
- 25 Garfinkel, C. I., and D. L. Hartmann, 2011: The influence of the quasi-biennial oscillation on the troposphere in wintertime in a hierarchy of models. Part I: Simplified dry GCMs. J. Atmos. Sci., 68, 1273–1289.
- Granger, C.W.J. Investigating causal relations by econometric models and cross-spectral methods, 37, 424-438 (1969) 648–650. *Econometrica*
- Gray, L. J., Beer, J., Geller, M., Haigh, J. D., Lockwood, M., Matthes, K., Cubasch, U., Fleitmann, D., Harrison, G., Hood, L., Luterbacher, J., Meehl, G. A., Shindell, D., Van Geel, B., and White, W.: Solar influence on climate, Rev. Geophys., 2010.
- 30 Haigh, J. D., and M. Blackburn (2006), Solar influences on dynamical coupling between the stratosphere and troposphere, Space Sci. Rev., 125, 331–344 ,
- Hendon, Harry H.; Abhik, S. Differences in Vertical Structure of the Madden-Julian Oscillation Associated With the Quasi-Biennial Oscillation. Geophysical Research Letters, v. 45, n. 9, p. 4419-4428, 2018.
- Hui, E. C., Chen, J. (2012). Investigating the change of causality in emerging property markets during the financial tsunami. Physica A: Statistical Mechanics and its Applications, 391(15), 3951-3962. *Physica A: Statistical Mechanics and its Applications.*
- 35 S. M. Kang, . Polvani, L. M , Fyfe, J.C. Sigmond, M., Impact of Polar Ozone Depletion on Subtropical Precipitation, Science 332, 951 (2011).



- KASAHARA, Akira; Puri, Kamal. Spectral representation of three-dimensional global data by expansion in normal mode functions. *Monthly Weather Review*, v. 109, n. 1, p. 37-51, 1981.
- Kidston, J., A. A. Scaife, S. C. Hardiman, D. M. Mitchell, N. Butchart, M. P. Baldwin, and L. J. Gray (2015), Stratospheric influence on tropospheric jet streams, storm tracks and surface weather, *Nat. Geosci.*, 8(6), 433–440, doi:10.1038/ngeo2424.
- 5 Kim, H., Caron, J. M., Richter, J. H., & Simpson, I. R. (2020). The lack of QBO-MJO connection in CMIP6 models. *Geophysical Research Letters*, e2020GL087295.
- Kitsios, V., O’kane, T. J., & Žagar, N. (2019). A Reduced-Order Representation of the Madden–Julian Oscillation Based on Reanalyzed Normal Mode Coherences. *Journal of the Atmospheric Sciences*, 76(8), 2463-2480.
- Li, K.-F., Tian, B., Waliser, D. E., Schwartz, M. J., Neu, J. L., Worden, J. R., and Yung, Y. L.: Vertical structure of MJO-related subtropical
10 ozone variations from MLS, TES, and SHADOZdata, *Atmos. Chem. Phys.*, 12, 425–436, 2012.
- LIU, Yuyun et al. Three Eurasian teleconnection patterns: Spatial structures, temporal variability, and associated winter climate anomalies. *Climate dynamics*, v. 42, n. 11-12, p. 2817-2839, 2014.
- Longuet-Higgins, Michael Selwyn. The eigenfunctions of Laplace’s tidal equation over a sphere. *Philosophical Transactions of the Royal Society of London. Series A, Mathematical and Physical Sciences*, v. 262, n. 1132, p. 511-607, 1968.
- 15 Lu, H., Scaife, A. A., Marshall, G. J., Turner, J., & Gray, L. J. (2017). Downward Wave Reflection as a Mechanism for the Stratosphere–Troposphere Response to the 11-Yr Solar Cycle. *Journal of Climate*, 30(7), 2395-2414.
- Lutkepohl, H. *New Introduction to Multiple Time Series Analysis*. (Springer, Berlin, 2005).
- Meehl, G. A., J. M. Arblaster, K. Matthes, F. Sassi, and H. vanLoon (2009), Amplifying the Pacific climate system response to a small 11-year solar cycle forcing, *Science*, 325, 1114–1118,
- 20 Massaroppe, Lucas; Baccala, Luiz A. Detecting nonlinear Granger causality via the kernelization of partial directed coherence. Rio de Janeiro, RJ: ISI-International Statistical Institute, 2015.
- Massaroppe, Lucas; Baccala, Luiz A. Kernel-nonlinear-PDC extends Partial Directed Coherence to detecting nonlinear causal coupling. In: 2015 37th Annual International Conference of the IEEE Engineering in Medicine and Biology Society (EMBC). IEEE, 2015. p. 2864-2867.
- 25 Marshall, A.G. Hedon, H.H. Hendon Son, S-W Lim, Y. Impact of the quasi-biennial oscillation on predictability of the Madden–Julian oscillation, *Clim Dyn* (2016).
- NAPPO, Carmen J. An introduction to atmospheric gravity waves. Academic press, 2013.
- Osprey, S. M., N. Butchart, J. R. Knight, A. A. Scaife, K. Hamilton, J. A. Anstey, V. Schenzinger, and C. Zhang, An unexpected disruption of the atmospheric quasi-biennial oscillation, 2016. *Science*
- 30 Percival, D.B. and Walden, A.T. *Spectral Analysis for Physical Applications: Multitaper and Conventional Univariate Techniques*. (Cambridge University Press, Cambridge, 1993). 23
- Raphaldini, B., Teruya, A. S., Silva Dias, P. L., Mayta, V.R. C., Takara, V.J. (2020), Normal mode perspective on the 2016 QBO disruption: Evidence for a basic state regime transition, *Geophysical Research Letters* (In press).
- Raupp, C. F., Silva Dias, P. L., Tabak, E. G., & Milewski, P. (2008). Resonant wave interactions in the equatorial waveguide. *Journal of the Atmospheric Sciences*, 65(11), 3398-3418.
- 35 Schelter, B., Winterhalder, M., Eichler, M., Peifer, M., Hellwig, B., Guschlbauer, B., Timmer, J. (2006). Testing for directed influences among neural signals using partial directed coherence. *Journal of neuroscience methods*, 152(1), 210-219.



- Sameshima, K., Baccala, L. A. (1999). Using partial directed coherence to describe neuronal ensemble interactions. *Journal of neuroscience methods*, 94(1), 93-103.
- SAMESHIMA, K.; TAKAHASHI, D. Y. ; BACCALÁ, L. A. . On the statistical performance of Granger-causal connectivity estimators. *Brain Informatics*, v. 2, p. 119-133, 2015.
- 5 Singh, S. V.; KRIPALANI, R. H.; SIKKA, D. R. Interannual variability of the Madden-Julian oscillations in Indian summer monsoon rainfall. *Journal of Climate*, v. 5, n. 9, p. 973-978, 1992.
- SUGIHARA, George et al. Detecting causality in complex ecosystems. *science*, v. 338, n. 6106, p. 496-500, 2012.
- Son, S.-W., Y. Lim, C. Yoo, H. H. Hendon, and J. Kim(2017): Stratospheric control of Madden-Julian Oscillation, *Journal of Climate*, 30, 1909-1922.
- 10 Takahashi, D.Y., Baccala, L.A. , Sameshima, K. Connectivity inference between neural structures via partial directed coherence. . 10, 1259-1273 (2007). *J. Appl. Stat.* ,
- Takahashi, Daniel Y.; Baccalá, Luiz A. ; Sameshima, Koichi . Information theoretic interpretation of frequency domain connectivity measures. *Biological Cybernetics* v. 103, p. 463-469, 2010.. *Biological cybernetics* ,
- Tirabassi, G., Sommerlade, L. and Masoller, C. Inferring directed climatic interactions with renormalized partial directed coherence and
15 directed partial correlation *Chaos* 27, 035815 (2017).
- Tian, B., Yung, Y., Waliser, D., Tyranowski, T., Kuai, L., Fetzer, E., and Irion, F.: Intraseasonal variations of the tropical total ozone and their connection to the Madden-Julian Oscillation, *Geophys. Res. Lett.*, 34, L08704, doi:10.1029/2007GL029451, 2007.
- van Loon, H., and G. A. Meehl (2012), The Indian summer monsoon during peaks in the 11 year sunspot cycle, *Geophys. Res. Lett.*, 39, L13701
- 20 Tirabassi, G., Sommerlade, L., & Masoller, C. (2017). Inferring directed climatic interactions with renormalized partial directed coherence and directed partial correlation. *Chaos: An Interdisciplinary Journal of Nonlinear Science*, 27(3), 035815.
- Wheeler, M.C. and Hendon, H. H., An All-Season Real-Time Multivariate MJO Index: Development of an Index for Monitoring and Prediction. *Mon. Wea. Rev.*, 132, 1917-1932, 2004.
- Yoo, C., and S.-W. Son (2016), Modulation of the boreal winter time Madden-Julian oscillation by the stratospheric quasi-biennial oscillation,
25 *Geophys. Res. Lett.*, 43, *Geophys. Res. Lett.*
- Wahl, Benjamin et al. Granger-causality maps of diffusion processes. *Physical Review E*, v. 93, n. 2, p. 022213, 2016.
- Žagar, N. et al. Normal-mode function representation of global 3-D data sets: open-access software for the atmospheric research community. *Geoscientific Model Development*, v. 8, n. 4, p. 1169-1195, 2015.
- Žagar, Nedjeljka; Frankze, Christian LE. Systematic decomposition of the Madden-Julian Oscillation into balanced and inertio-gravity components. *Geophysical Research Letters*, v. 42, n. 16, p. 6829-6835, 2015.
- 30 Zhang, Chidong. Madden-Julian oscillation. *Reviews of Geophysics*, v. 43, n. 2, 2005.
- ZHANG, Chidong; ZHANG, Bosong. QBO-MJO Connection. *Journal of Geophysical Research: Atmospheres*, v. 123, n. 6, p. 2957-2967, 2018.
- ZHANG, Taotao et al. The weakening relationship between Eurasian spring snow cover and Indian summer monsoon rainfall. *Science advances*, v. 5, n. 3, p. eaau8932, 2019.
- 35

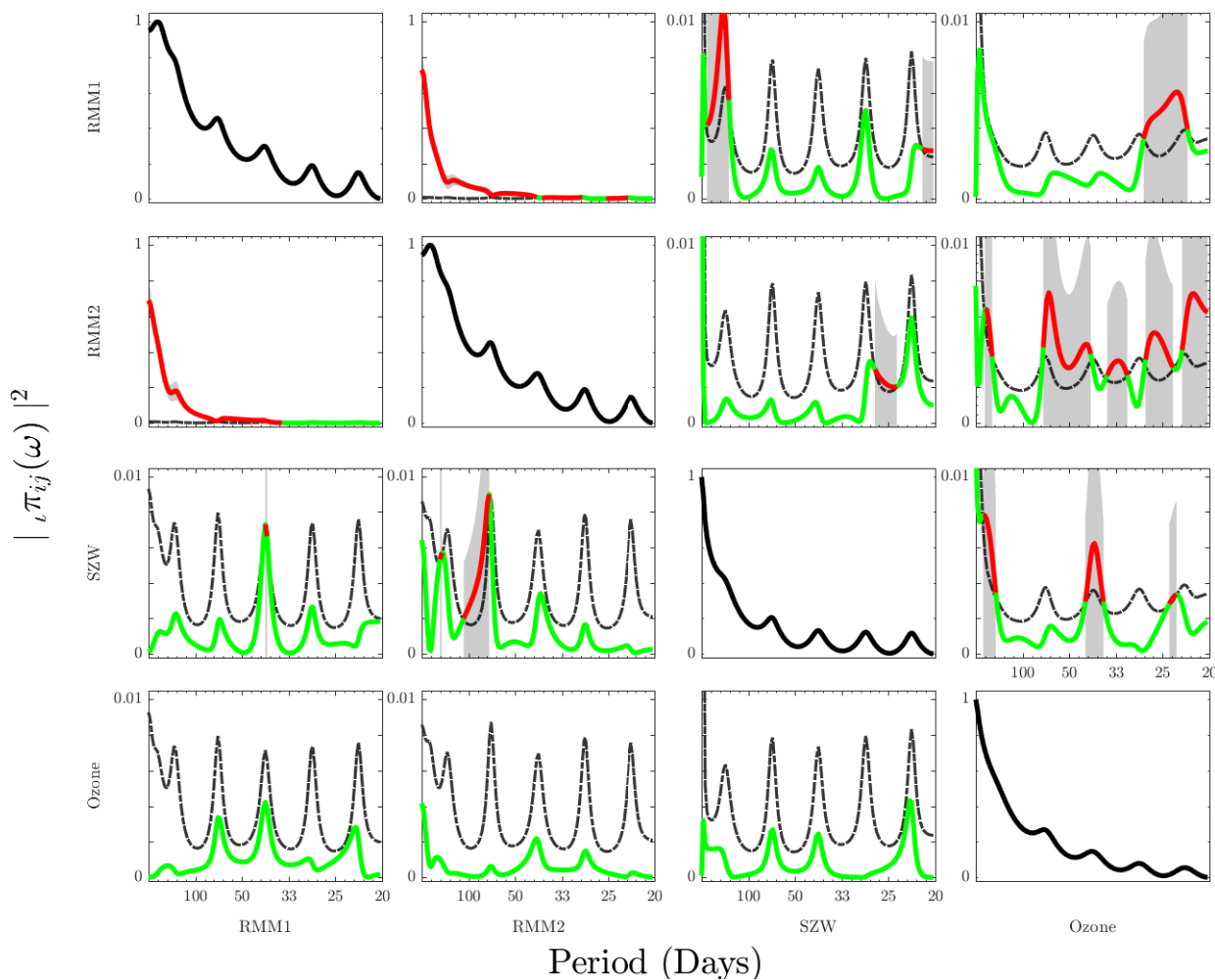


Figure 1. PDC analysis at the fast (>20 days) timescale, colored (red/green) curve represents the PDC value, green for not statistically significant causality at that period and red for significant causality with 95% confidence level, the dashed line represents the threshold for statistical significance. The PDC plot is read as causality from the variable on the horizontal to the variable on the vertical (see details on the supplementary material). Pictures on the diagonal represent the power spectrum of the variable.

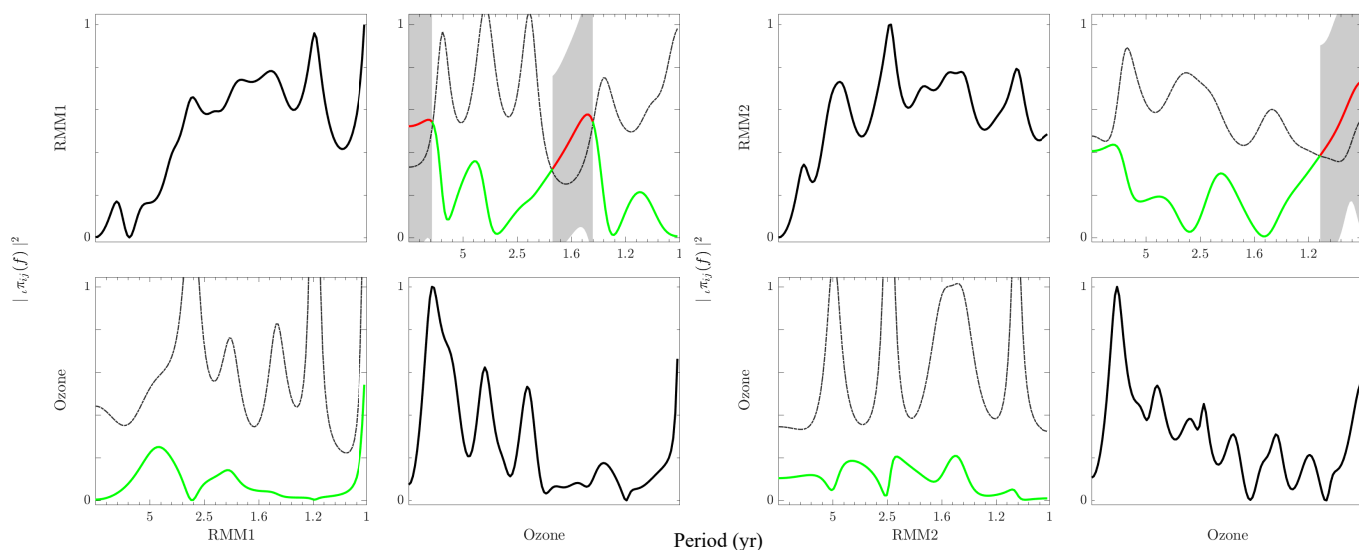


Figure 2. PDC between tropical stratospheric ozone and MJO at the slow (>1yr) timescale, periods given are given in years. Ozone is found to significantly cause RMM1 on periods of 1.5-2 yr and on the decadal timescale.

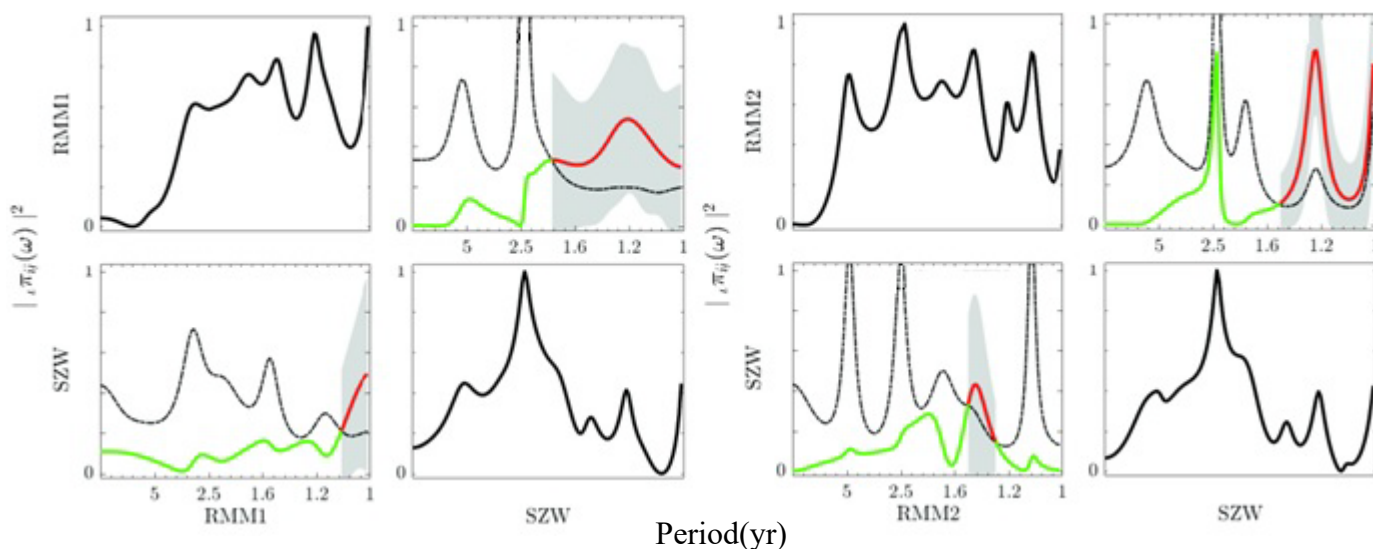


Figure 3. PDC analysis between MJO and Stratospheric zonal winds (SZW) at the slow (>1 year periods) timescale. Results indicate significant interaction on the annual-biennial timescales.

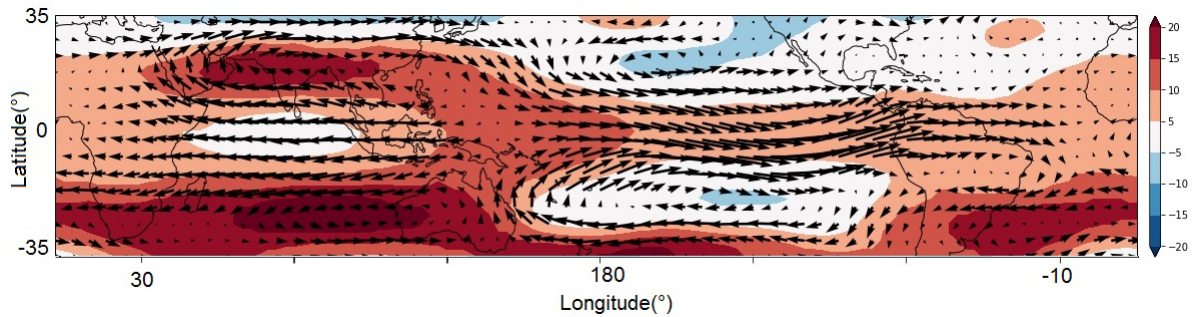


Figure 4. horizontal velocity and pressure fields reconstructed by inverting the selected MJO-related modes in agreement with (Zagar & Frankze, 2015).

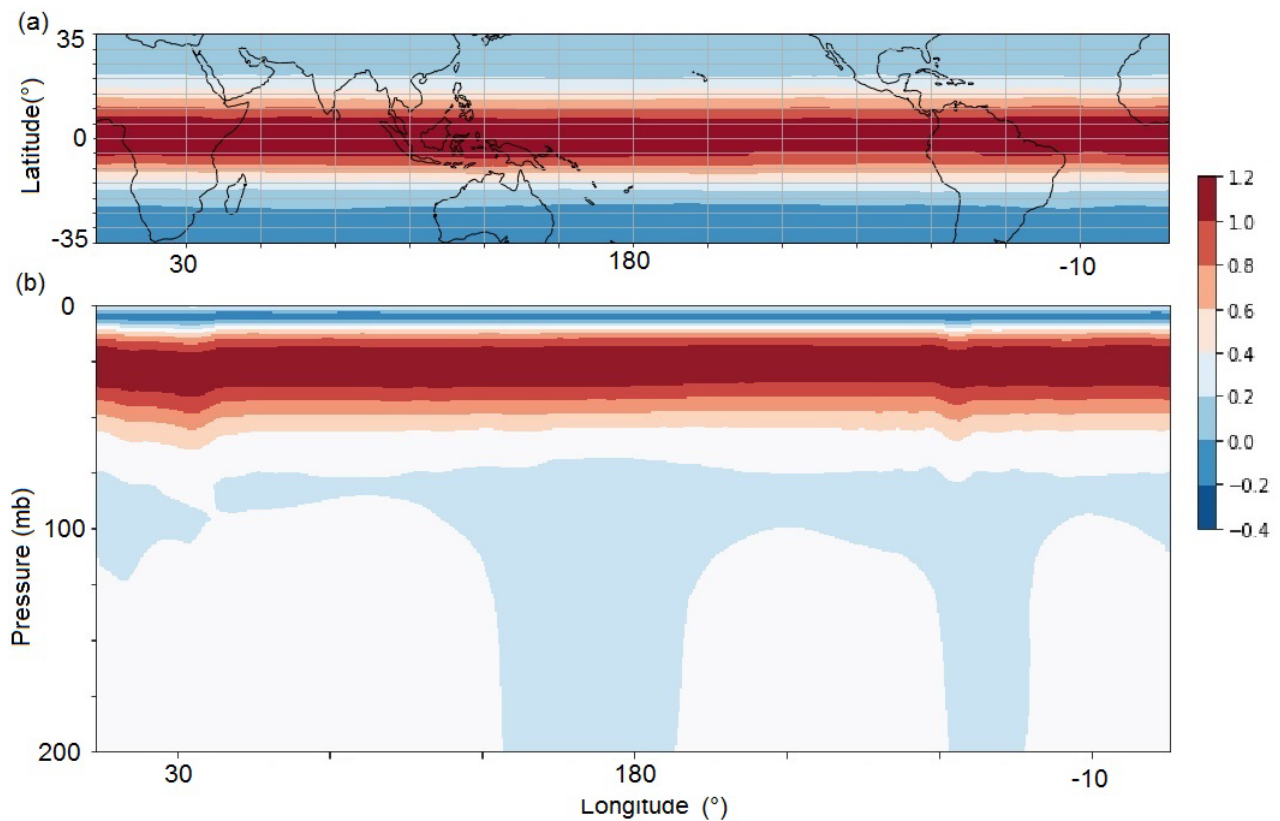


Figure 5. Zonal velocity field of the inversion of the QBO-related modes in a horizontal plane at 29mb (a) and at an equatorial vertical cut (b) showing the equatorial zonal wind structure concentrated in the stratosphere.

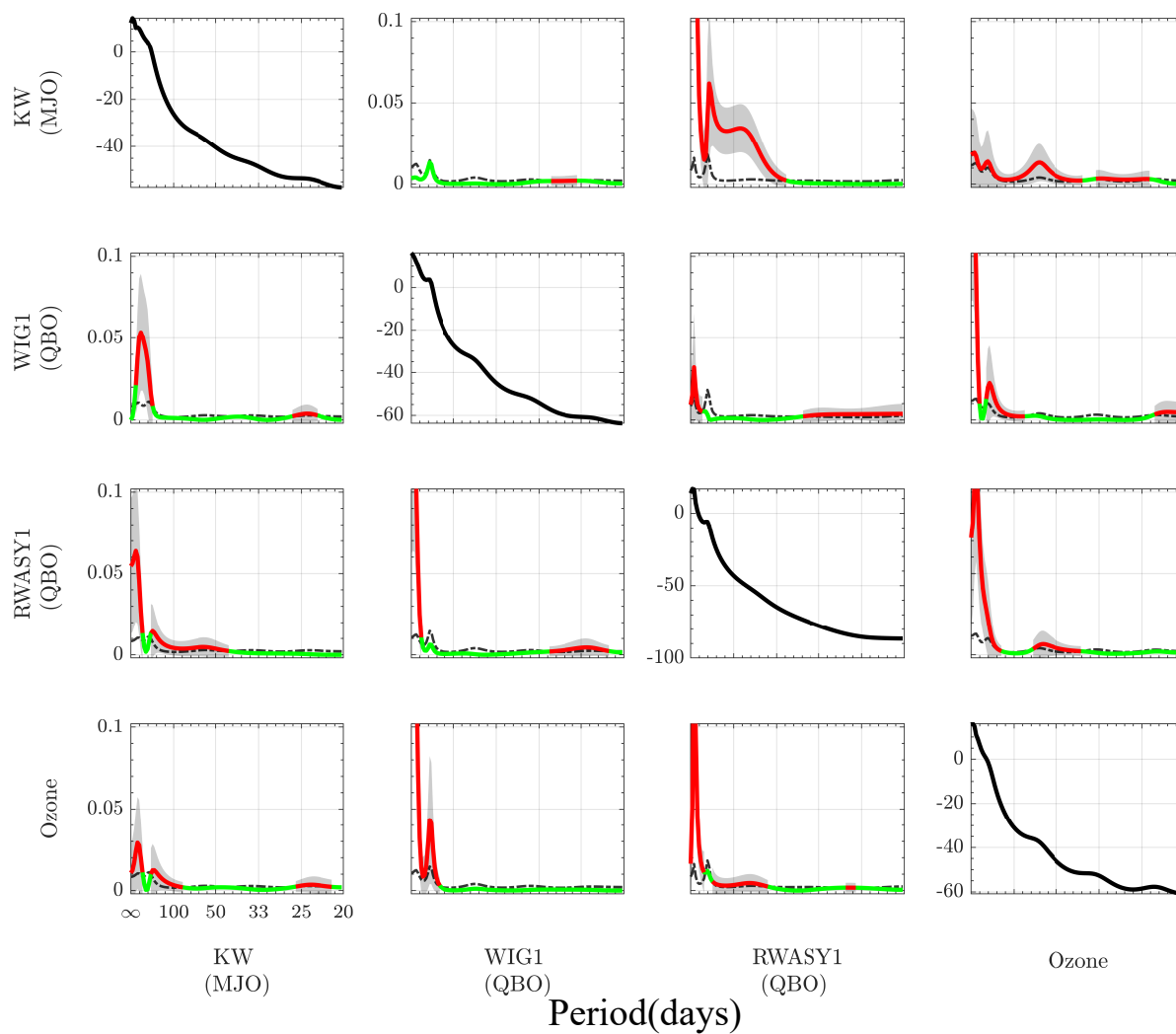


Figure 6. PDC analysis of the interaction of Kelvin, asymmetric Rossby, westward gravity modes and ozone at the fast timescale. Significant interactions (red curve) between MJO and ozone/QBO-related modes is found on intraseasonal, semi-annual and annual time-scales.

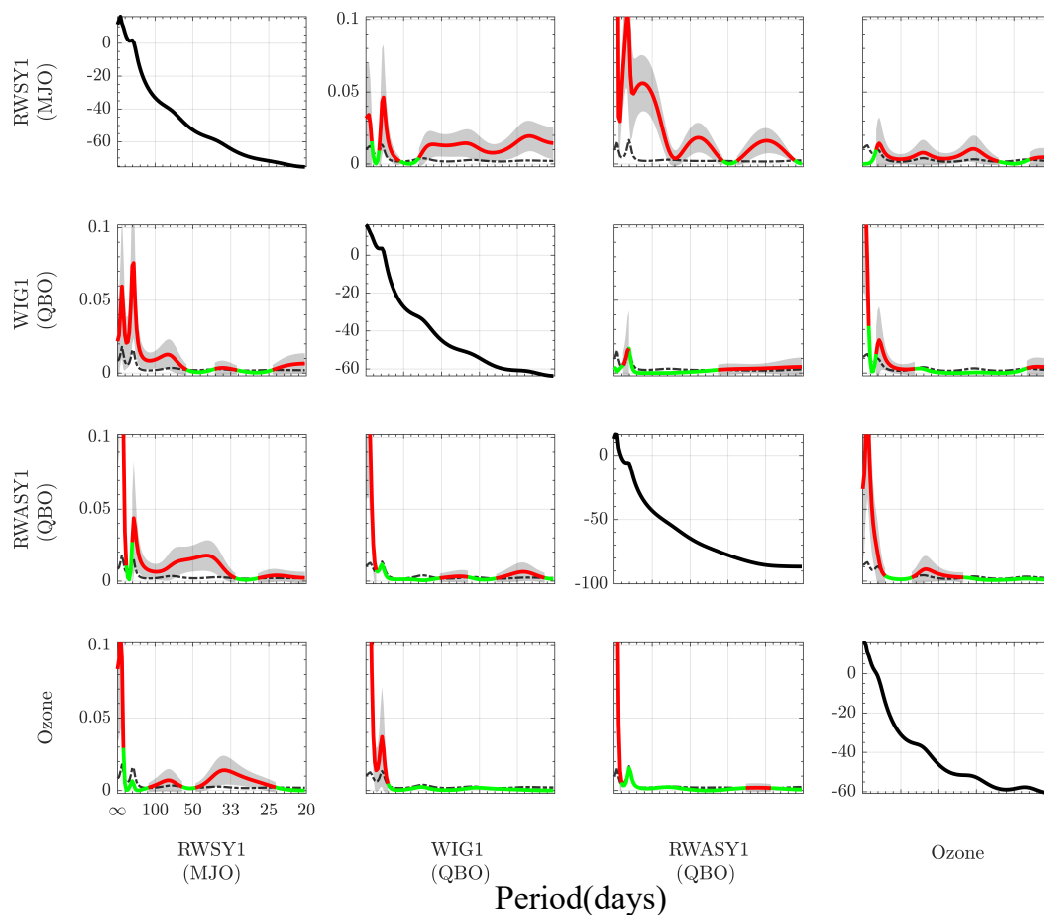


Figure 7. PDC analysis of the interaction of symmetric Rossby 1, asymmetric Rossby 1 and westward gravity modes and ozone at the fast timescale. Again, significant interactions (red curve) between MJO and ozone/QBO-related modes is found on intraseasonal, semi-annual and annual time-scales.

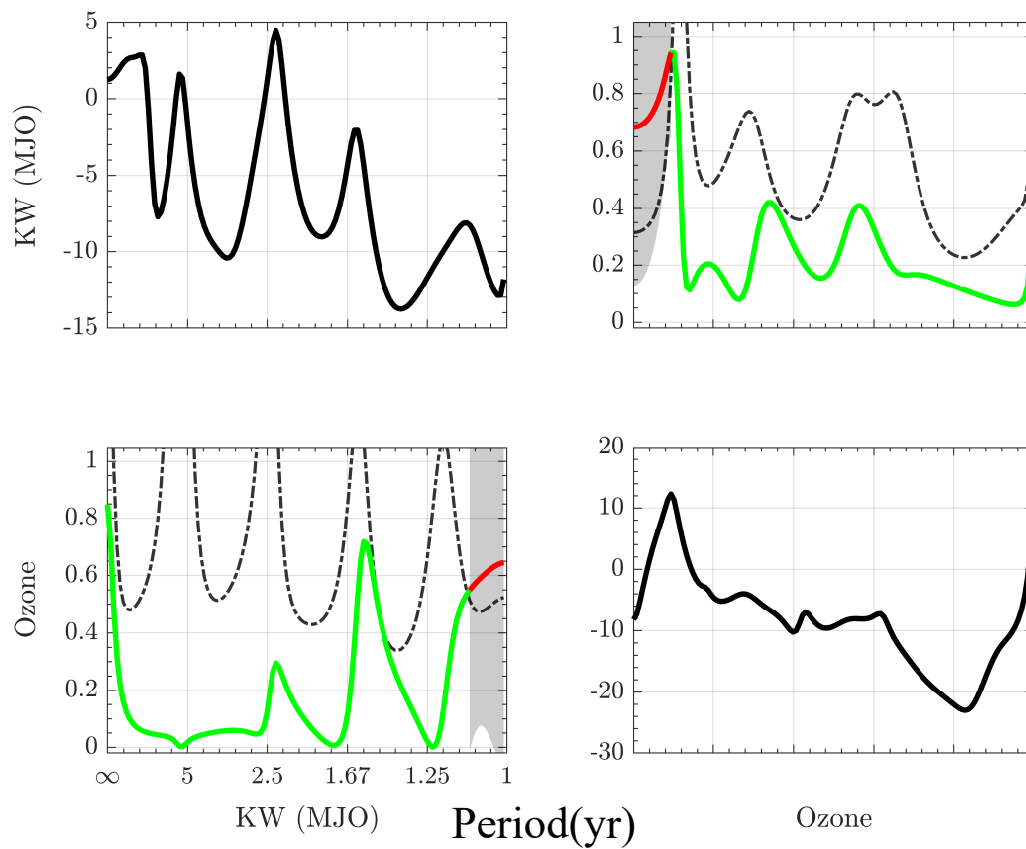


Figure 8. PDC analysis of the interaction of Kelvin modes and Kelvin waves (KW) at the slow timescale. The results show that KW influence the ozone on the annual time-scale, while the ozone influences KW on decadal time-scales.

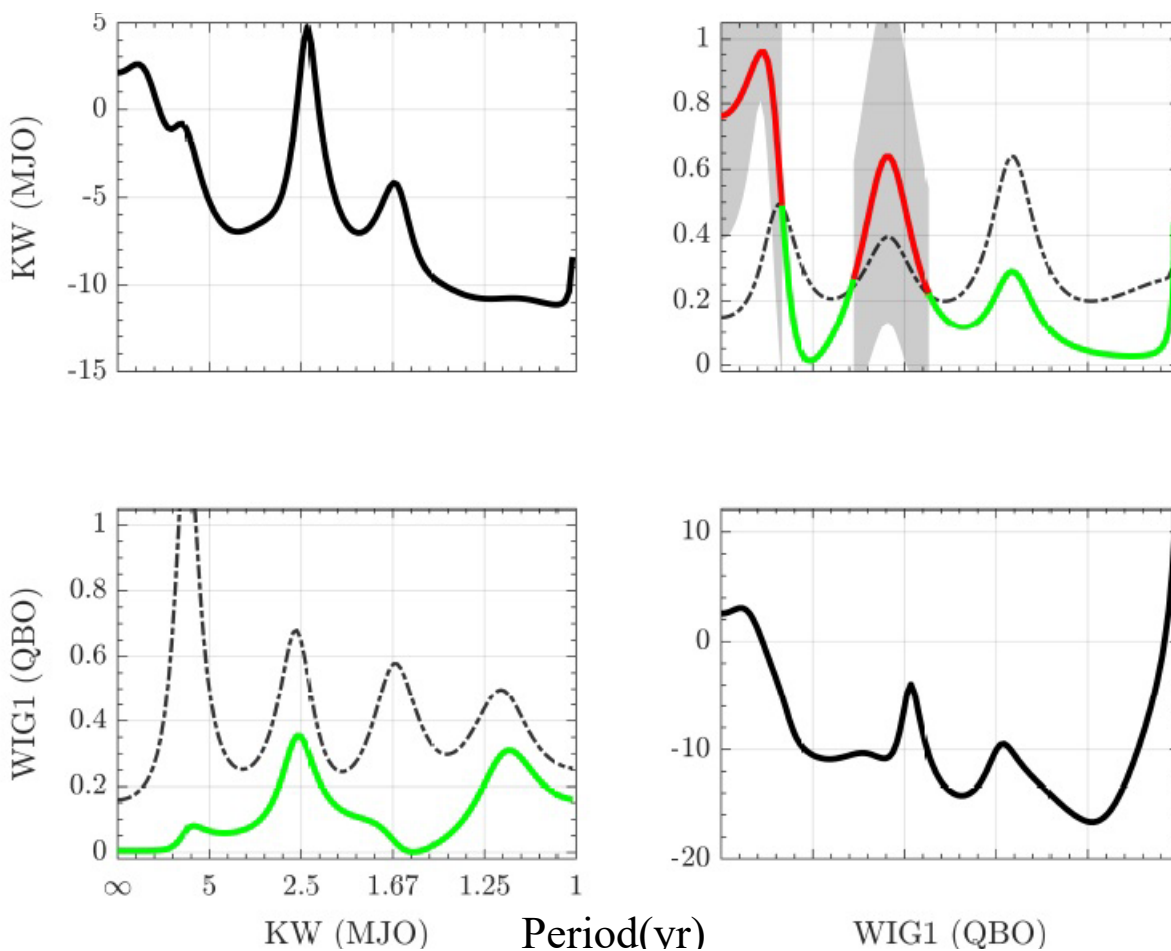


Figure 9. PDC analysis of the interaction of Kelvin modes (KW) and westward gravity modes (WIG) at the slow timescale. The results show a strong influence of the WIG mode on the KW on biennial and decadal timescales.

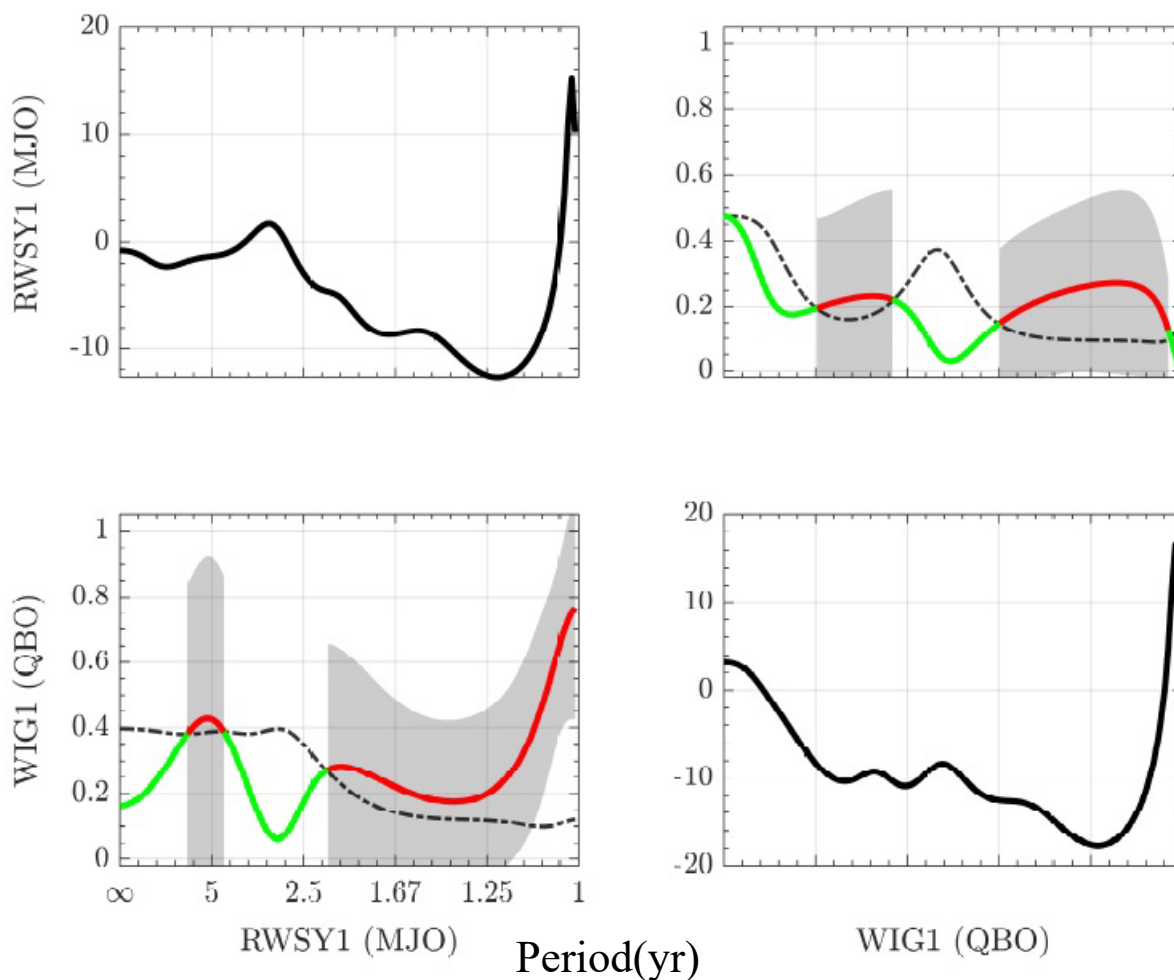


Figure 10. PDC analysis of the interaction of symmetric Rossby modes (meridional index 1, denoted by RWSY1) and westward gravity modes (WIG1) at the slow timescale. Important interactions are found in annual to interannual time-scales.

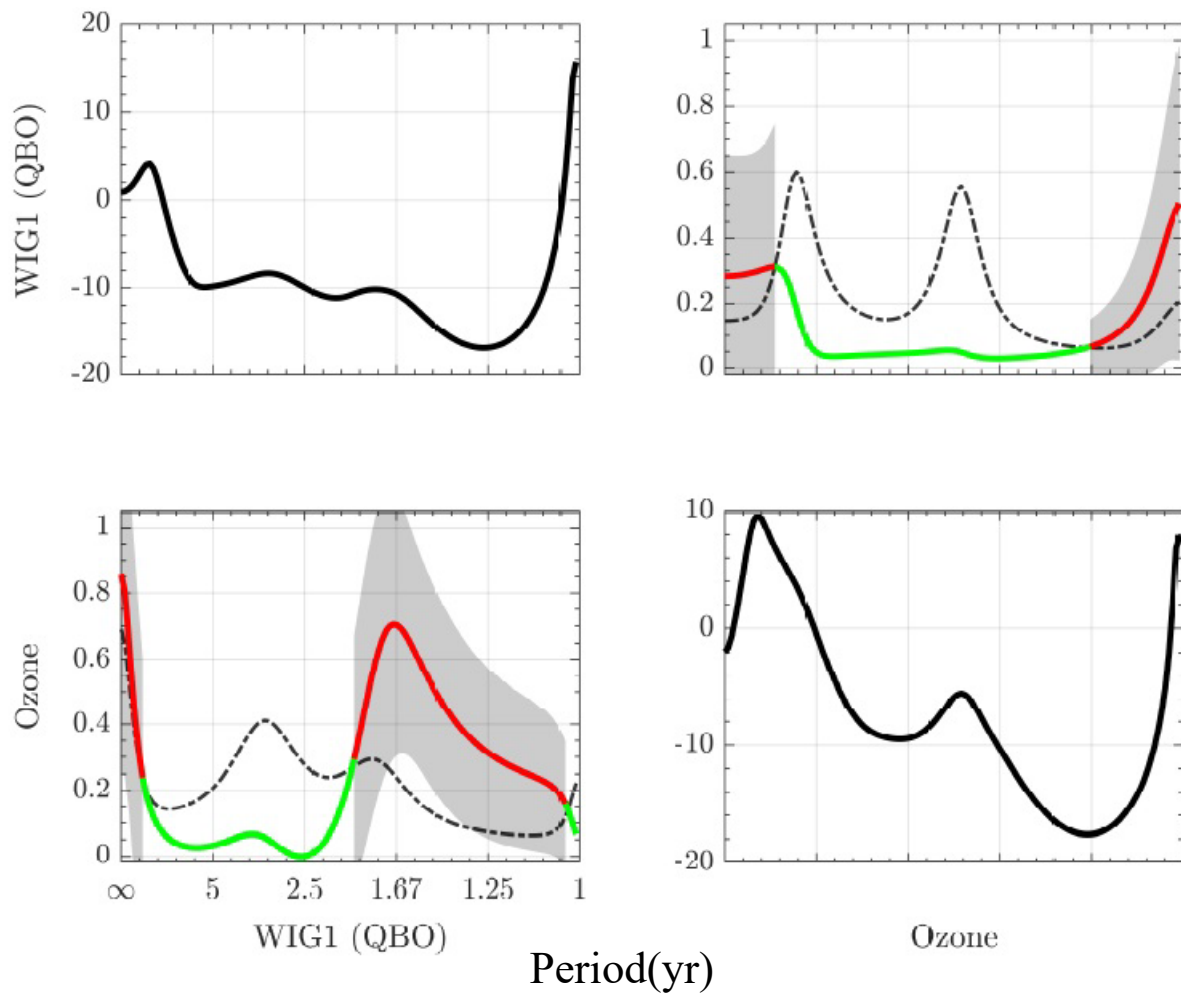


Figure 11. PDC analysis of the interaction of westward gravity modes and ozone at the slow timescale. Important interactions are found on annual-biennial times-scales as well as on the decadal time-scale.

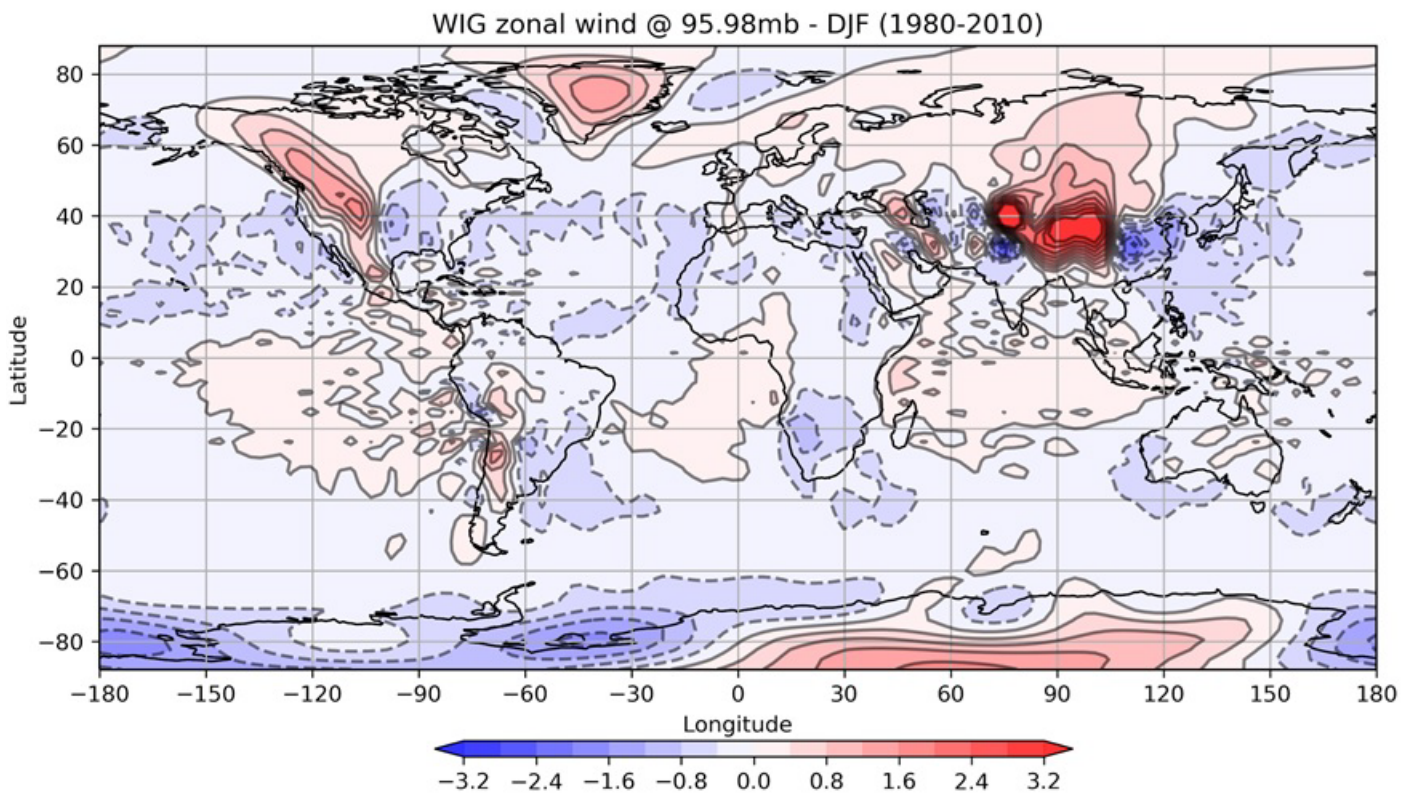


Figure 12. Spatial (horizontal) structure of the zonal wind (in m/s) associated with the westward inertio gravity waves with vertical wave-number 1-4.

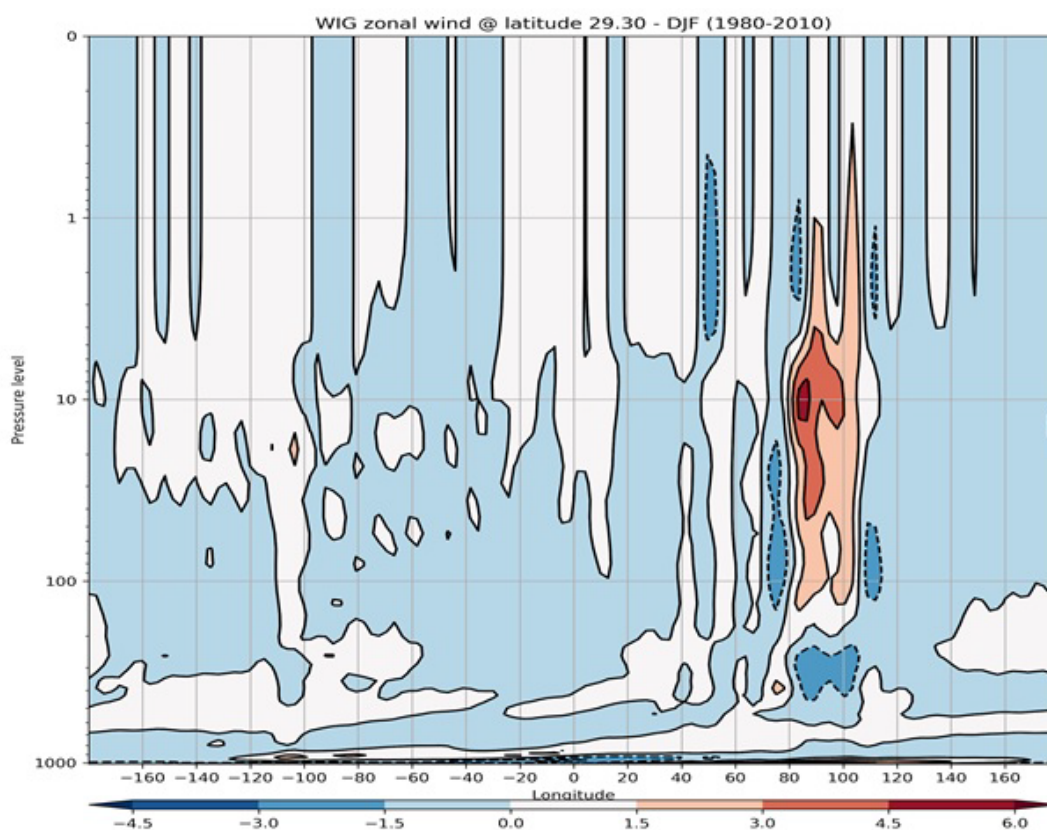


Figure 13. Spatial structure (vertical) of the zonal wind (in m/s) associated with the westward inertia gravity waves with vertical wave-number 1-4.